Rev. Roum. Sci. Techn.– Électrotechn. et Énerg.
Vol. **63**, *1*, pp. 100–105, Bucarest, 2018

SENSORLESS FIELD ORIENTED CONTROL OF CURRENT SOURCE INVERTER FED INDUCTION MOTOR DRIVE

HAMZA FEROURA*, FATEH KRIM, BILLEL TALBI, ABDELBASET LAIB, ABDESSLAM BELAOUT

Key words: Current source inverter (CSI), Direct filed oriented control (DFOC), Model predictive control (MPC).

This paper aims to present a speed sensorless direct field oriented control (DFOC) of an induction motor (IM) fed by current source inverter (CSI). The DFOC is based on the orientation of the rotor flux to be superposed on the d axis of the rotating frame (dq), to achieve similar performances of those of dc motors, hence, the flux is controlled by the d axis current and the torque by the q axis current separately. The stator currents and voltages are employed for the estimation of the rotor flux and its angle and then the calculation of the rotation speed, by means of a sliding mode observer (SMO). Unlike voltage source inverters, a capacitive filter is required at the output of the CSI for current commutation and harmonics filtering, the mathematical model of this filter is used for the prediction and the control of the motor voltages. Simulation results under MATLAB/Simulink have been obtained to verify the effectiveness of the different proposed strategies.

1. INTRODUCTION

The induction motor associated with power electronic converters constitute variable speed drives whose the industrial use is in incessant growing. These motors are rugged, reliable, economical, and suitable for low and medium power variable speed drives [1].

Despite these advantages, the non-linear relation between the magnetic flux and the electromagnetic torque renders the control of this type of motors complex [1,2]. To overcome this drawback, control strategies have been designed, such like scalar control with voltage to frequency constant ratio, direct torque control (DTC) which controls directly the motor torque through a look up table, and the field oriented control (FOC) strategy which can control the induction motor with same performances as the dc motors.

The FOC is a powerful control method. It has the advantage of controlling independently the flux and the torque, which means that the torque variation is achieved with constant flux and vice-versa. Consequently the system will be linear and easy to control [2].

Induction motors are usually fed by voltage source inverters (VSI), principally because of their simplicity of dc supply and due to their developed voltage and current control strategies. But they have also drawbacks such like high common mode component, acoustic noise, and large dv/dt voltage transitions due to pulse width modulated (PWM) voltages and this may cause deterioration of the motor windings [2–4]. However, CSI as compared with VSI in the field of speed control of ac drives, offers many features such as reliability, ruggedness, inherent short circuit protection, capability of four-quadrant operation without extra regeneration power circuit, and motor friendly currents and voltages with low dv/dt resulting from filtering effect of the output capacitor filter [1–3].

There are several modulation techniques for CSI, among them trapezoidal PWM (TPWM) technique which the dual technique of VSI PWM. The pulse patterns calculated offline with selective harmonic elimination (SHE) is also one the most used strategies to control the CSI mainly because of the low harmonic content it offers. Another widespread technique is current space vector modulation (SVM) which is very used due to its simplicity of implementation. And recently appeared a new control strategy, named finite-set model predictive control (FS-MPC), which is a promising advanced control method that explicitly uses the system's model to predict its future changes [3]. The basic idea of MPC is the determination of the required control signals in advance. It calculates at each sampling period all the possible current vectors and selects the optimal one by means of an optimization cost function.

Induction motor drives require often information about the rotation speed for the regulation, by using sensor for this purpose. Nevertheless, the presence of speed sensor increases the system cost, and the complexity of the installation and reduces the reliability due to the high sensibility and delicacy of such sensor to external disturbances.

Recent researches about CSI fed IM drives were mostly focused on control strategies, PWM techniques, and sensorless speed operation. In [4] an improved direct torque control (DTC) strategy based on the orientation of the stator flux has been proposed to overcome the drawback of variable switching frequency. The authors in [5] used shunt active power filters to enhance the power quality at both input and output terminals. [6] proposes a hybrid control strategy for the CSI based on SVM, and SHE. Common mode voltage reduction using MPC scheme is proposed in [7], and harmonics interaction suppression in [8, 9]. Current controller design has been proposed in [10] using two decoupling methods in the synchronous reference frame. In [11] a modified vector control strategy is proposed by adding two current control loops. Sensorless techniques of IM drives are proposed in [12–14]

This paper proposes an improved DFOC strategy (Fig. 1) with extra current regulation loops, based on a novel model predictive voltage control (MPVC) technique for CSI using an adaptive SMO for speed estimation.

This paper is divided into seven sections. Following the introduction in Section 1, the modelling of the IM is presented in Section 2. In Section 3 the DFOC strategy is illustrated. The basics of the speed SMO are discussed in Section 4. Section 5 presents the principle of the proposed MPVC strategy. Simulation results are shown and discussed in Section 6. And finally the conclusion forms Section 7.

University of Setif, Department of Electronics, LEPCEI Laboratory, 1, 19000 Setif, Algeria, E-mail: hamzaferoura@hotmail.com

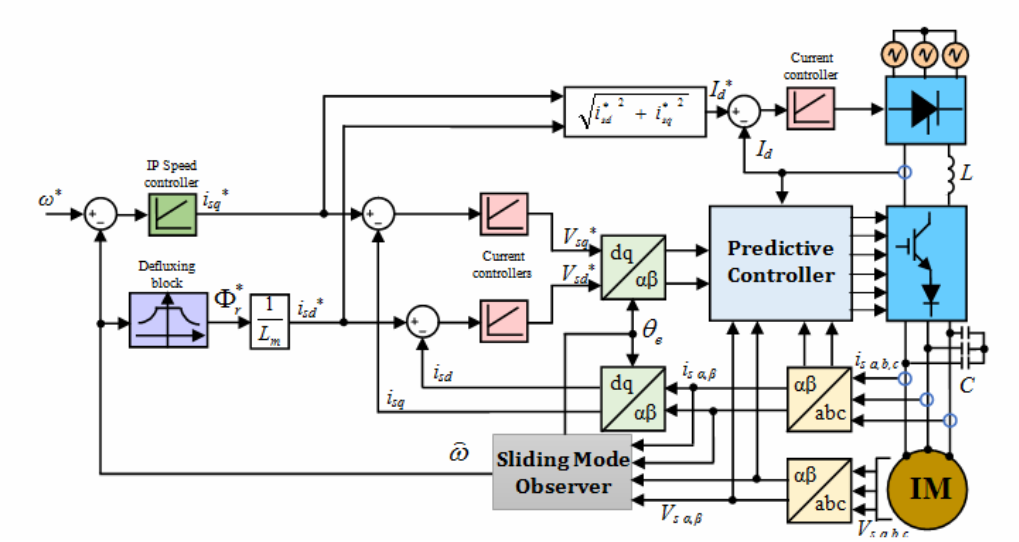

Fig. 1– Block diagram of the proposed CSI fed DFOC-IM drive.

2. INDUCTION MOTOR MODEL

Assuming linear magnetic circuits, equal mutual inductances and neglecting core saturation and iron losses, the squirrel-cage IM dynamic model can be represented by a well-known set of complex equations in a synchronously rotating frame

$$\vec{v}_s = R_s\vec{i}_s + \frac{d\vec{\phi}_s}{dt} + j\omega_s\vec{\phi}_s \quad (1)$$

$$0 = R_r\vec{i}_r + \frac{d\vec{\phi}_r}{dt} + j(\omega_s - \omega_r)\vec{\phi}_r \quad (2)$$

$$\vec{\phi}_s = L_s\vec{i}_s + L_m\vec{i}_r \quad (3)$$

$$\vec{\phi}_r = L_r\vec{i}_r + L_m\vec{i}_s \quad (4)$$

$$T_e = \frac{3pL_m}{2L_r}\cdot \Im m(\vec{\phi}_r'\cdot\vec{i}_s)\,, \quad (5)$$

where $\vec{v}_s$ and $\vec{i}_s$ are the stator voltage and current vectors respectively, $\vec{i}_r$ is the rotor current vector , $\vec{\phi}_s$ and $\vec{\phi}_r$ are the stator and rotor flux vectors respectively, ω_s and ω_r are stator and rotor field speeds respectively, R_s and R_r are the stator and rotor resistances respectively, L_s, L_r and L_m are the stator, rotor, and magnetizing inductances, respectively, T_e and p are electromagnetic torque and number of pole pairs, respectively, and $\vec{\phi}_r'$ is the complex conjugate value of the rotor flux vector .

3. DIRECT FIELD ORIENTED CONTROL

Using a proper field orientation, the stator current can be decomposed into flux producing component and torque producing component, then these two components are controlled separately [2].

In this work, the rotor flux orientation is used for the control of the induction machine. It is achieved by aligning the d-axis of synchronous rotating frame with the rotor flux vector $\vec{\phi}_r$ as shown in Fig. 2.

$$\phi_{rq} = 0 \text{ and } \phi_{rd} = \phi_r = \text{const}\,. \quad (6)$$

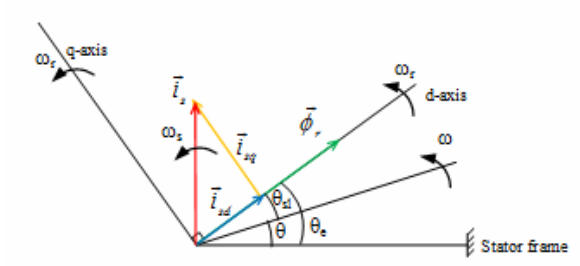

Fig. 2 – Field orientation in the synchronous rotating frame.

From (5) the electromagnetic torque is given by

$$T_e = \frac{3pL_m}{2L_r}\cdot(\phi_{rd}\cdot i_{sq} - \phi_{rq}\cdot i_{sd})\,. \quad (7)$$

From the equations (2–4)

$$-R_r\frac{L_m}{L_r}i_{sd} - (\omega_s - \omega_r)\phi_{rq} + \frac{R_r}{L_r}\phi_{rd} + \frac{d\phi_{rd}}{dt} = 0\,. \quad (8)$$

Taking into account that rotor flux is kept constant equal to its reference. Substituting (6) into (7) and (8) yields

$$T_e = \frac{3pL_m}{2L_r}\cdot\phi_r^*\cdot i_{sq}\,. \quad (9)$$

So, the current references are as follows

$$i_{sq}^* = \frac{2L_r}{3pL_m\cdot\phi_r^*}\cdot T_e^*\,, \quad (10)$$

$$i_{sd}^* = \frac{\phi_r^*}{L_m}\,. \quad (11)$$

Two current control loops are designed using proportional-integrator (PI) regulators to generate the reference voltage, while an integrator- proportional (IP) regulator is used for the control of the rotation speed, as shown in Fig. 3.

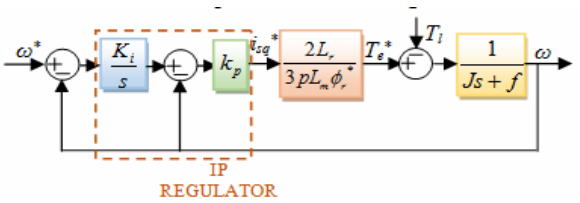

Fig. 3 –Speed control loop using IP regulator.

The rotor flux angle θ_e used for field orientation can be determined directly from measured stator voltages and currents, or from motor rotating speed and calculated slip angle θ_{sl} in the case of indirect FOC.

In this paper, the rotor flux, and its angle θ_e, and also the speed rotation are determined by an adaptive full-order SMO.

4. SLIDING MODE OBSERVER

The adaptive flux observers are now receiving considerable attention and many achieving new solutions because of their high precision and relative robustness gainst machine parameter deviation [2].

By means of the IM mathematical model, and using the sliding mode theory, the proposed full-order SMO can be modeled as follows

$$\frac{\mathrm{d}}{\mathrm{d}t}\hat{\phi}_s = V_s - R_s.i_s + k.\mathrm{sgn}(i_s - \hat{i}_s) \tag{12}$$

$$\frac{\mathrm{d}}{\mathrm{d}t}\hat{\phi}_r = \frac{L_m}{\tau_r}.i_s - \frac{1}{\tau_r}.\hat{\phi}_r + j.\hat{\omega}.\hat{\phi}_r + k'.\mathrm{sgn}(i_s - \hat{i}_s) \tag{13}$$

$$\hat{i}_s = \frac{1}{\sigma.L_s}\hat{\phi}_s - \frac{L_m}{\sigma L_s L_r}\hat{\phi}_r\,, \tag{14}$$

where (^) denotes an estimated value, $\sigma = 1-(L_m^2/L_sL_r)$, $\tau = L_r/L_m$, and k, k' are SMO gains.

The sliding surface (S) is constructed using the error between the measured and the estimated current $(i_s - \hat{i}_s)$. In this SMO a saturation function is used instead of the sign function to reduce the undesirable problem of chattering. The applied saturation function is defined below, where Δ is tuning parameter (Fig. 4)

$$\mathrm{Sat}(S) = \begin{cases} 1 & \text{if} \quad x - \hat{x} > \Delta \\ x - \hat{x}/\Delta & \text{if} \quad -\Delta < x - \hat{x} < \Delta \\ -1 & \text{if} \quad x - \hat{x} < -\Delta \end{cases}. \tag{15}$$

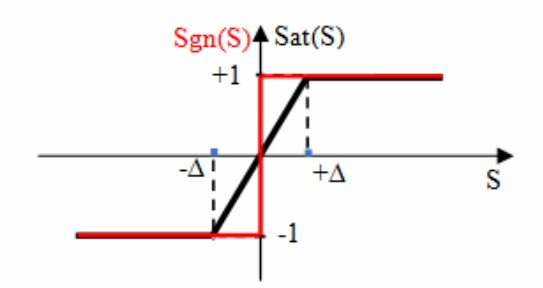

Fig. 4 – Sign and saturation SMO functions.

Using the estimated flux components, the synchronous speed can be calculated as

$$\hat{\omega}_r = \frac{\mathrm{d}}{\mathrm{d}t}\tan^{-1}\left(\frac{\hat{\phi}_{r\beta}}{\hat{\phi}_{r\alpha}}\right). \tag{16}$$

By consequence the slip speed ω_{sl} is deducted as

$$\hat{\omega}_{sl} = \frac{2.R_r}{3.P}\frac{\hat{T}_e}{\hat{\phi}_r^2}\,. \tag{17}$$

Thus, the below equation gives the estimated speed

$$\hat{\omega} = \hat{\omega}_r - \hat{\omega}_{sl}\,. \tag{18}$$

5. PREDICTIVE VOLTAGE CONTROL FOR CSI

The PWM CSI shown in Fig. 5 is composed of a current source (I_d), six unidirectional switches (IGBT in series with a diode), and a capacitive filter.

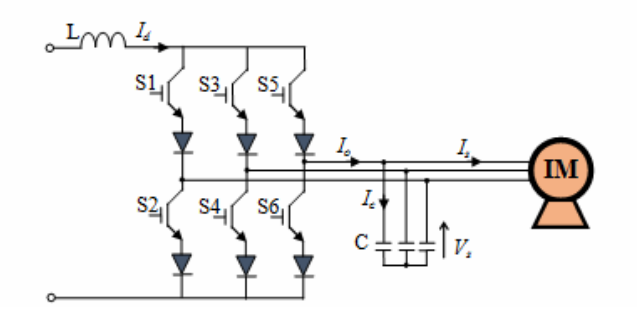

Fig. 5 – CSI-fed IM.

At any given time, the CSI must have at least one of the upper switches and one of the lower switches conducting simultaneously to ensure a current path for the dc-current.

In addition, only one of the upper and lower devices can conduct at a time to ensure the output current waveform. These restrictions can be summarized as follows

$$S_1 + S_2 + S_3 = S_2 + S_4 + S_6 = 1\,. \tag{19}$$

The output currents can be defined according to the switching signals and the dc-current I_d by

$$I_{oa} = (S_1 - S_2)I_d \tag{20}$$

$$I_{ob} = (S_3 - S_4)I_d \tag{21}$$

$$I_{oc} = (S_5 - S_6)I_d\,. \tag{22}$$

The valid switching states with the corresponding phase and output currents are presented in Table 1.

Table 1

Rules for mathematical symbols and equations

Switches						Phase current			Current vector
1	2	3	4	5	6	I_{La}	I_{Lb}	I_{Lc}	
1	0	0	0	0	1	I_{dc}	0	$-I_{dc}$	$\vec{i}_1 = 2I_{dc}\mathrm{e}^{(\mathrm{j}\pi/6)}/3^{1/2}$
0	0	1	0	0	1	0	I_{dc}	$-I_{dc}$	$\vec{i}_2 = 2I_{dc}\mathrm{e}^{(\mathrm{j}\pi/2)}/3^{1/2}$
0	1	1	0	0	0	$-I_{dc}$	I_{dc}	0	$\vec{i}_3 = 2I_{dc}\mathrm{e}^{(\mathrm{j}5\pi/6)}/3^{1/2}$
0	1	0	0	1	0	$-I_{dc}$	0	I_{dc}	$\vec{i}_4 = 2I_{dc}\mathrm{e}^{(\mathrm{j}7\pi/6)}/3^{1/2}$
0	0	0	1	1	0	0	$-I_{dc}$	I_{dc}	$\vec{i}_5 = 2I_{dc}\mathrm{e}^{(\mathrm{j}3\pi/2)}/3^{1/2}$
1	0	0	1	0	0	I_{dc}	$-I_{dc}$	0	$\vec{i}_6 = 2I_{dc}\mathrm{e}^{(\mathrm{j}11\pi/6)}/3^{1/2}$
1	1	0	0	0	0	0	0	0	$\vec{i}_7 = 0$
0	0	1	1	0	0	0	0	0	$\vec{i}_8 = 0$
0	0	0	0	1	1	0	0	0	$\vec{i}_9 = 0$

And the output current vectors are shown in Fig. 6.

The mathematical model of the output filter is

$$\vec{i}_o = C\frac{\mathrm{d}\vec{V}_s}{\mathrm{d}t} + \vec{i}_s\,, \tag{23}$$

where C is the filter capacitance, i_o the converter output current vector, V_s is the load output voltage vector and is the motor current vector.

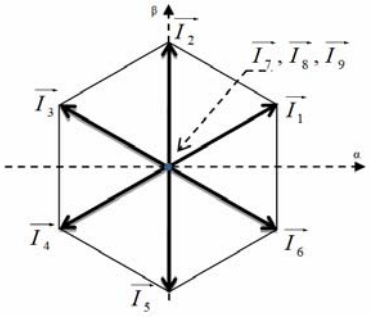

Fig. 6 – CSI output current vectors.

The space vector of the output voltages is given by

$$V_s(t) = \frac{2}{3}(v_{sa} + e^{2\frac{\pi}{3}j} v_{sb} + v_{sc} e^{-2\frac{\pi}{3}j}) \quad (24)$$

V_s can be expressed in the following form

$$V_s = v_{s\alpha}(t) + j v_{s\beta}(t) = V_s(t) e^{j\omega t} \quad (25)$$

where V_s is the instantaneous amplitude of the output voltages defined as

$$V_s(t) = \sqrt{(v_{s\alpha}^2 + v_{s\beta}^2)} \quad (26)$$

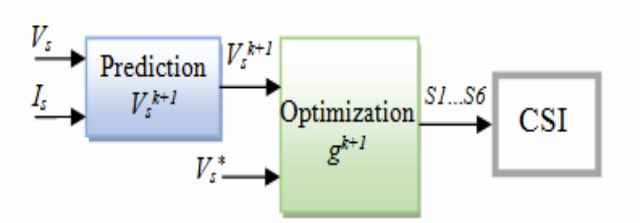

Fig. 7 – Predictive control scheme.

In Fig. 7, the proposed predictive voltage control is shown, which constitutes the major contribution of this work. The basic principle of this technique is the prediction of the future behavior of the controlled variables. The optimization criterion of the control method is expressed as a cost function to be minimized [3].

A. Prediction model. In this structure, the load currents, and voltages, are measured. These measures are necessary to predict the behavior of the controlled variables, which is the motor voltage. Then, based on this prediction, a cost function is minimized and the appropriate current vector is selected. Thus, the selection generates pulses to control the power switches of the inverter. The control algorithm is illustrated in Fig. 8.

For the prediction model an approximation in the discrete-time is considered, such as for a generic variable x [3]

$$\frac{dx}{dt} \approx \frac{x(k+1) - x(k)}{T_s}, \quad (27)$$

where T_s is the discrete-time sample time.

By the application of the approximation in equation (27) into equation (23), the discrete stator current can be written

$$i_o[k] = C\left(\frac{V_s[k+1] - V_s[k]}{T_s}\right) + i_s[k]. \quad (28)$$

From (28), the nine voltage predictions can be obtained as follows

$$V_s[k+1] = \frac{T_s}{C}(i_o[k] - i_s[k]) + V_s[k]. \quad (29)$$

B.Cost function. The nine prediction of the stator voltage are evaluated using a cost function g given by

$$g_i = \left\| V_s^* - V_s(k+1) \right\|. \quad (30)$$

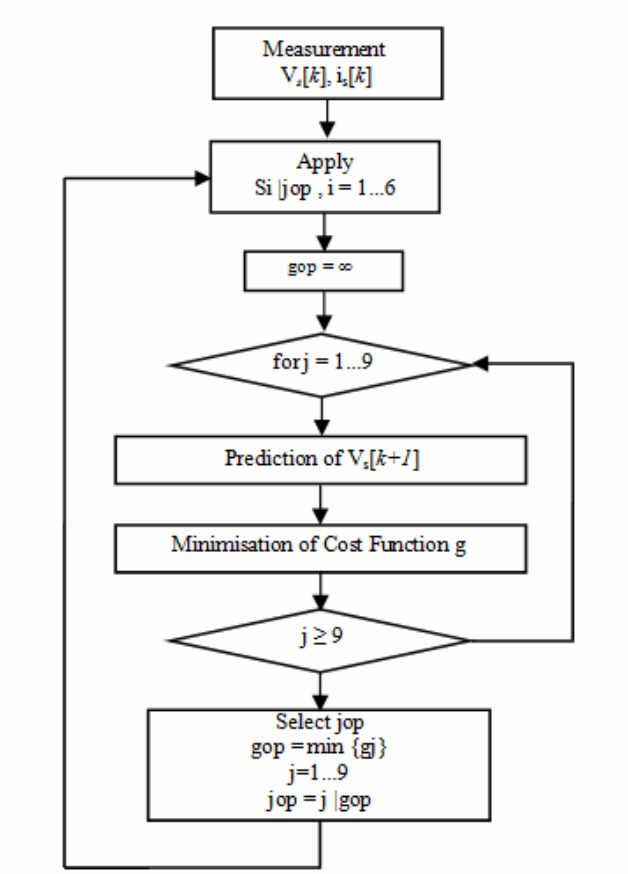

Fig. 8 – Predictive control algorithm.

6. SIMULATION RESULTS AND DISCUSSION

In order to evaluate the performance of the proposed SMO sensorless MPC based DFOC shown in Fig. 1, computer simulations using MATLAB/Simulink® have been performed using a low power induction motor of 0.37 kW whose parameters are listed in Table 2.

First the motor is started without mechanic load with speed reference of 100 Rad/s, and after 0.2 s, a rated load of 2.6 Nm is applied, in 0.4 s the motor is unloaded again.

A test of inversion of the rotation direction is done at 0.5 s. Finally at 0.7 s the speed reference is set to 40 rad/s to test the low speed operation of the proposed control strategy.

Fig. 9a shows both measured and observed rotation speeds. It is obvious that the speed follows rapidly the set reference during all the performed tests without overshoot and static error.

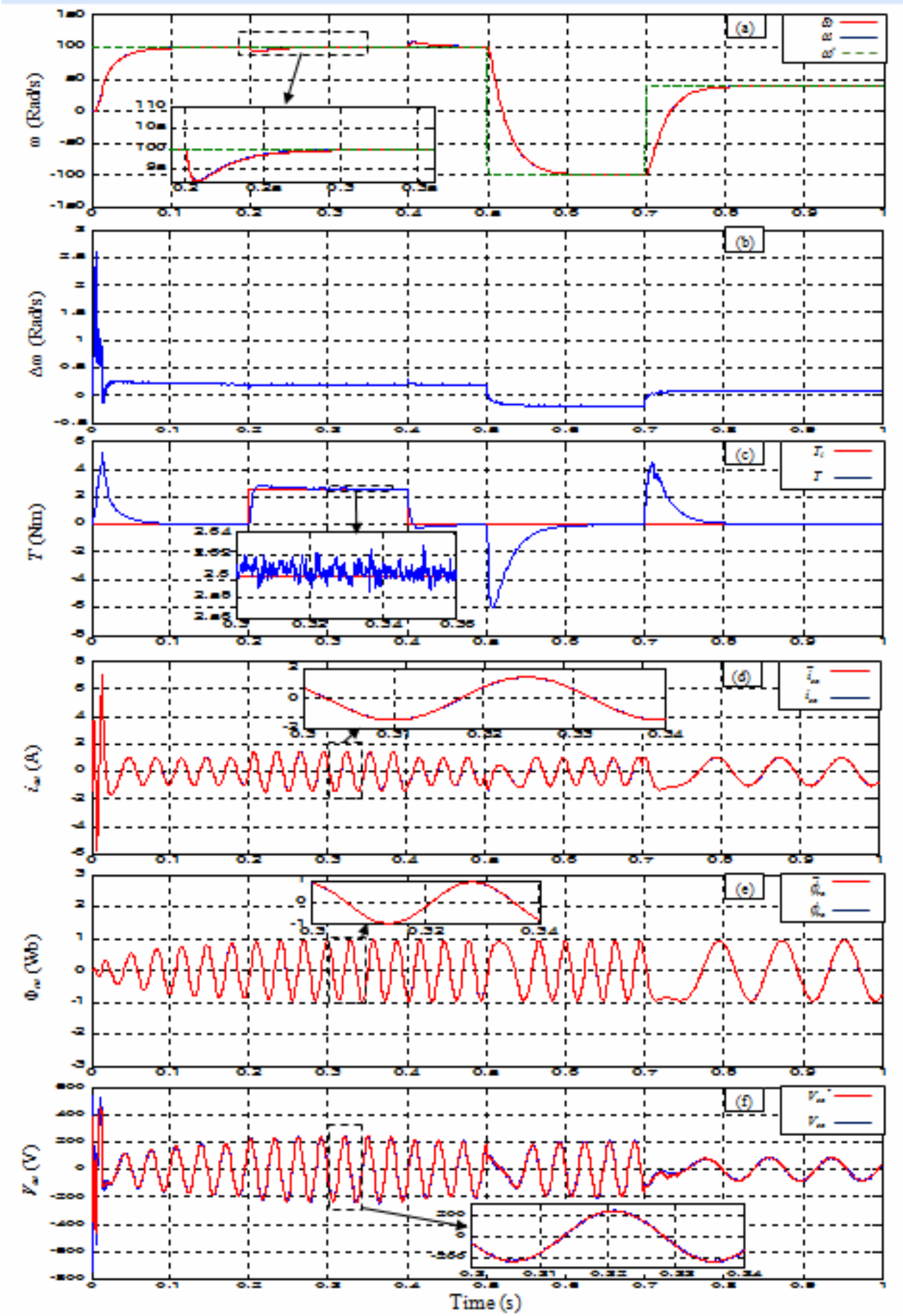

Fig. 9 – DFOC responses of CSI-Fed IM:
a) rotation speed; b) speed observation error; c) electromagnetic torque; d) stator current; e) rotor flux; f) stator voltage.

This explains the use of the IP regulator instead of the conventional PI. It is also notable that the measured and the observed speeds are practically identical, as shown in Fig. 9b. The error between the two speeds is approximately neglected.

In Fig. 9c the torque response is given, it is remarkable that it responds swiftly with low ripple about 0.04 Nm as shown in the zoom.

The measured and the observed currents of motor's phase (a) are represented in Fig. 9d, it can be seen that the current is practically sinusoidal with low total harmonic distortion (THD = 0.51 %). Furthermore the observed current is superposed on the measured one.

The same thing can be seen in the waveforms of the rotor flux, Fig. 9e where the observed and the measured waveforms are identical, and the value of the flux is kept constant at the rated value of 0.95 Wb during all the simulated tests.

Figure 9f exhibits the effectiveness of the MPVC method, the motor voltage follows the reference perfectly with very low distortion.

Table 3 presents a comparison between the proposed MPVC based DFOC in this paper, and some other control techniques achieved in the field ac drives.

Table 2

Simulated drive parameters

Rated power	$P = 0.37$ kW
Stator resistance	$R_s = 20.2\ \Omega$
Rotor resistance	$R_r = 14.45\ \Omega$
Stator inductance	$L_s = 0.982$ H
Rotor inductance	$L_r = 0.982$ H
Mutual inductance	$L_m = 0.921$ H
Rated voltage	$V_s = 220/380$ V
Number of pole pairs	$p = 2$
Rated speed	$N = 1385$ rpm
Rated torque	$T = 2.6$ N.m
Moment of inertia	$J = 0.00095$ kg.m^2
Friction coefficient	$f = 0.00001$ N.m/s
dc link inductor	$L = 10$ mH
CSI output capacitor filter	$C = 5\ \mu$F
Sample time	$T_s = 40\ \mu$s

Table 3

Comparison of different control techniques

	FOC of VSI fed IM	DTC of CSI fed IM	SVM based FOC of CSI fed IM	SHE based FOC of CSI fed IM	Proposed MPVC based FOC of CSI fed IM
Current THD	Low	Medium	Low	Extremely low	Very low
Voltage THD	Very High	Medium	Low	Low	Low
Torque ripple	Small	Very Large	Moderate	Small	Very small
Response	Fast	Slow	Medium	Slow	Fast

7. CONCLUSIONS

In this paper, a new DFOC strategy for an IM supplied by a CSI has been proposed and simulated in MATLAB/ Simulink®. This strategy is based on a novel MPC technique to control the motor voltages by using extra current regulation loops to generate the reference voltages, where the output capacitive filter is used as a model for predictions.

A full-order SMO has been proposed to estimate the rotor flux, and the rotation speed without sensors. In the addition an IP type regulator is introduced and preferred in comparison with a simple PI regulator to have a fast response and overshoot suppression.

Performance results presented in the previous Section, show the good performances of the proposed DFOC based on MPVC in terms of fast response and motor currents and voltages, where the waveforms are close to sinusoidal with very low harmonic distortion.

The proposed technique is simple and easy to implement, future research is open to test robustness against parameters sensitivity and measurement errors for SMO and predictive controller, and to consider the use of intelligent controllers.

Received on December 17, 2016

REFERENCES

1. B.K. Bose, *Modern power electronics and AC drive*, Prentice Hall PTR, Inc., New Jersey, USA, 2002.
2. H. Abu-rub, I. Atif, J. Guzinski, *High performance control of AC drive with Matlab/Simulink models*, John Wiley & Sons Ltd., New Jersey, USA, 2012.
3. J. Rodriguez, P. Cortes, *Predictive control of power converters and electrical drives*, John Wiley & Sons Ltd., New Jersey, USA, 2012.
4. M. Babaei, H. Heydari, *Direct Torque Control of Pulse Width Modulation Current Source Inverter-fed Induction Motor by Novel Switching Method*, Electric Power Components and Systems, **38**, *5*, pp. 514–532 (2010).
5. A. Shehada, A.R. Beig, *An improved CSI fed induction motor drive*, Electrical power and energy systems, **46**, pp. 26–35 (2013).
6. Z. Wang, B. Wu, D. Xu, N. R. Zargari, *Hybrid PWM for High-Power Current-Source-Inverter-Fed Drives With Low Switching Frequency*, IEEE Transactions on Power Electronics, **26**, *6*, pp. 1754–1764 (2011).
7. H. Gao, B. Wu, D. Xu, M. Pande, R.P. Aguilera, *Common-Mode Voltage Reduced Model Predictive Control Scheme for Current Source Converter-Fed Induction Motor Drives*, IEEE Transactions on Power Electronics, **32**, *6*, pp. 4891–4904 (2017).
8. Y. Zhang, Y.W. Lei, *Investigation and Suppression of Harmonics Interaction in High-Power PWM Current-Source Motor Drives*, IEEE Transactions on Power Electronics, **30**, *2*, pp. 668–679 (2015).
9. J. Yong, X. Li, D. Xu, W. Xu, *Interharmonic Source Model for Current Source Inverter Fed Variable Frequency Drive*, IEEE Transactions on Power Delivery, **32**, *2*, pp. 812–821 (2017).
10. H. J. Lee, S. Jung, S. K. Sul, *A Current Controller Design for Current Source Inverter-Fed AC Machine Drive System*, IEEE Transactions on Power Electronics, **28**, *3*, pp. 1366–1381 (2010).
11. A.K. Abdelsalam, M.I. Masoud, M.S. Hamad, B.W. Williams, *Modified Indirect Vector Control Technique for Current-Source Induction Motor Drive*, IEEE Transactions on Industry Applications, **48**, *6*, pp. 2433–2442 (2012).
12. M. Morawiec, *Sensorless control of induction motor supplied by current source inverter*, Asian Journal of Control, **18**, *2*, pp. 1–6 (2013).
13. A. Ahriche, M. Kidouche, A. Idir, Y. Deia, *Combinig sliding mode and second lyapuniv function for flux estimation*, Rev. Roum. Sci. Techn. – Électrotechn. et Énerg., **61**, *2*, pp. 106–110 (2016).
14. A.K. Abdelsalam, M.I. Masoud, M.S. Hamad, B.W. Williams, *Improved Sensorless Operation of a CSI-Based Induction Motor Drive: Long Feeder Case*, IEEE Transactions on Power Electronics, **28**, *8*, pp. 4001–4012 (2013).